Iranian Journal of Veterinary Science and Technology

Received: 2025- May-27
Accepted after revision: 2025- Nov-18
Published online: 2025- Nov-18

RESEARCH ARTICLE

DOI: 10.22067/ijvst.2025.93653.1549

Characterization and phylogenetic analysis of a mitochondrial targeting alpha/beta hydrolase protein in *Strongyloides ratti*

Abbas Jolodar

Department of Basic Sciences, Biochemistry and Molecular Biology Section, Faculty of Veterinary Medicine, Shahid Chamran University of Ahvaz, Ahvaz, Iran.

ABSTRACT

Strongyloides ratti is widely used as an experimental model for studying and diagnosing humans strongyloidiasis. The alpha/beta hydrolase domain proteins are ubiquitously distributed across all organisms. In this study, a 780-nucleotide cDNA fragment was amplified by RT-PCR, and BLAST analysis revealed that 98.54% sequence identity with the only incomplete S. ratti mRNA sequence available in GenBank (XM_024652394.1). Using this fragment as a probe, two expressed sequence tags (ESTs), 856 bp (FC815910.1) and 526 bp (BI742498.1), corresponding to the 3'and 5' ends, respectively, were identified and assembled into a full length cDNA of 919 bp, designated SrABH. Its amino acid sequence exhibited 97.98% identity with the only available *S. ratti* sequence in GenBank (XP_024505975.1). The molecular weight (MW) and isoelectric point (pI) of the protein are 33.484 kDa and 7.18, respectively. Signal peptide analysis indicated the absence of a secretion signal, however a mitochondrial targeting cleavage site was identified between amino acids 21-22. The highly conserved motif consists of nine amino acids spanning positions 111 to 120. The 3D structural analysis revealed that SrABH consists of 9 alpha-helices (39.18%), 8 beta-sheets (18.21%), and loop regions (42.61%). Phylogenetic analysis clustered SrABH with related nematode sequences, displaying by a high bootstrap support of 98. The lowest genetic distance (0.01%) was observed between SrABH and the only sequence isolated from *S. ratti* (XP_024505975.1). Given its molecular characteristics, this parasite's data may be valuable in structure-based drug design strategies using *S. ratti* as a model system for the human pathogen *S. stercoralis*.

Keywords

Esterase, alpha/beta hydrolase domain, Strongyloides ratti, RT-PCR, mitochondria

Number of Figures: 6
Number of Tables: 1
Number of References: 31
Number of Pages: 10

Abbreviations

S. ratti : Strongyloides ratti

S. stercoralis: Strongyloides stercoralis

Corresponding authors: *Abbas Jolodar*
Email: jolodara@scu.ac.ir
Tel: +98(61)3333-0073

Introduction

Strongyloides is a genus of gastrointestinal nematodes of medical and veterinary importance, infecting a wide range of mammalian species, encompassing both humans and other animals. Among these species, *Strongyloides ratti* is closely related to the human parasite *S. stercoralis* and has therefore been widely adopted as a robust experimental model for investigatinFg the *S. stercoralis*. The infective third-stage larvae of *S. ratti* actively penetrate the skin of their rodent hosts and subsequently migrate to the mucosal lining of the small intestine, where they mature into adult worms. Hatched eggs and first-stage larvae are then released into the environment through fecal excretion [1].

Strongyloidiasis typically presents with mild symptoms; however, its clinical manifestations can become severe in individuals receiving immunosuppressive drugs, undergoing organ transplantation, or suffering from malignancies and malnutrition, all of which are linked to immunodeficiency. *S. stercoralis* is a human-specific parasite and is endemic in tropical and subtropical regions worldwide. Due to its close evolutionary relationship with *S. stercoralis*, *S. ratti*, has been frequently used as a laboratory model for studying *Strongyloides* treatment, diagnostics and genetic mapping [2, 3].

Alpha/beta hydrolase domain protein-encoding genes are present in nearly all sequenced genomes. This enzyme family has rapidly become one of the largest structural groups, exhibiting diverse catalytic functions in various biological processes, including parasite-host interactions. Despite their ubiquity, the substrates and metabolic pathways of these enzymes remain poorly characterized. A defining feature of this enzymes family is the presence of a conserved catalytic triad composed of Nucleophilic-Histidine-Acidic residue, which enables efficient process of substrates with diverse chemical compositions and physicochemical properties in various biological settings. Structurally, these proteins are similar and highly conserved across evolution, and play critical roles in energy metabolism, cell signaling, and growth and development [4]. This family includes a wide range of esterases, which include enzymes such as acetylcholinesterase, dienolactone hydrolase, lipase, thioesterase, serine carboxypeptidase, proline iminopeptidase, proline oligopeptidase, haloalkane dehalogenase, haloperoxidase, epoxide hydrolase, and hydroxynitrile lyase.

This protein has been identified in the excretory/secretory materials of parasitic nematodes, including *Haemonchus contortus* [5], *Heligmosomoides polygyrus* [6], and *Mesocestoides corti* [7]. Similar proteins have also been detected in free-living and parasitic organisms, such as *Caenorhabditis elegans* [8], the thioesterase type II enzyme from *Cryptosporidium parvum* [9], and the lysophospholipase from *Schistosoma japonicum* [10]. Beyond parasites, this protein and its homologues, including ABHD5 and ABHD11, have been reported in *Arabidopsis thaliana* [11, 12] and in *Saccharomyces cerevisiae* [13]. Members of this protein family are thus broadly distributed across eukaryotic species, including the Ndr1 protein in *Helianthus annuus* (common sunflower), known as Sf21.

In this study, we aimed to perform a computational characterization and phylogenetic analysis of an alpha/beta hydrolase domain-containing gene from *S. ratti*, given its close genetic relationship with the human pathogen *S. stercoralis*.

Results

Amplification of the SrABH sequence was performed by RT-PCR, using cDNA as a template and two gene specific primers. The PCR reaction yielded a single product of approximately 800 bp, as confirmed by agarose gel electrophoresis (Figure 1). Sequencing analysis demonstrated that this fragment corresponded to a portion of the central region of the alpha/beta hydrolase gene. A BLASTn search against the GenBank database revealed that the amplified product shared 98.54% sequence identity with the only incomplete *S. ratti* mRNA sequence available (XM_024652394.1), covering approximately 95% of the overlapping regions. To obtain the full-length cDNA sequence, the amplified fragment was used as a probe to search the

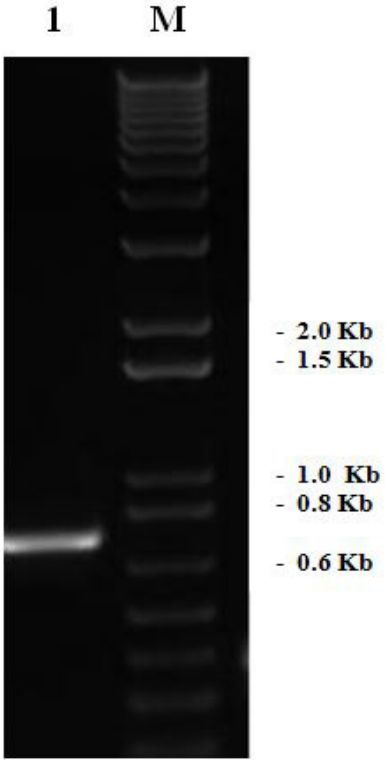

Figure 1. Agarose gel electrophoresis of RT-PCR products from infective S. ratti larvae. M: DNA size marker. Lane 1: RT-PCR amplification products.

Expressed Sequence Tags (EST) database. Two ESTs were identified: FC815910.1 (856 bp), corresponding to the 3' end, and BI742498.1 (526 bp), corresponding to the 5' ends of the gene. Assembly of these EST sequences and determining its overlapping regions, allowed reconstruction of a complete Open Reading Frame (ORF), which was designated SrABH.

The assembled cDNA sequence measured 919 bp, containing an ATG start codon at position 1 and a TAG stop codon at position 871. A 43-nucleotides 3' untranslated region (UTR) was identified downstream of the stop codon (Figure 2). The predicted

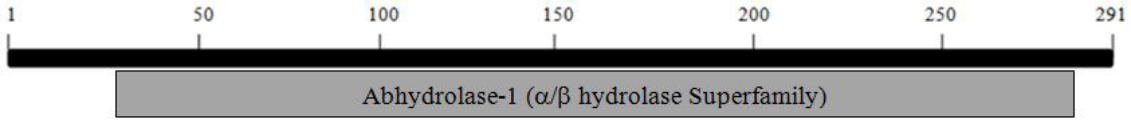

Figure 2.
Visual representation of the SrABH domain.
.

protein sequence of this fragment, consists of 291 amino acids encoded by a complete open reading frame (ORF). Analysis of amino acid composition revealed that the protein contains aliphatic (22%), aromatic (11%), positively charged (15%), and negatively charged (12%) residues. Leucine was the most abundant amino acid, with 32 residues (11%), whereas tryptophan was the least abundant, with 2 residues (0.69%). The predicted molecular weight of the protein was determined to be 33.484 kDa, with the isoelectric point (pI) of 7.18. SignalP analysis indicated the absence of a signal peptide . ScanProsite analysis identified a highly conserved motif in the SrABH protein consists of nine amino acids (DLLGHSMGG) located between residues 112 and 120, with a serine residue precisely positioned at amino acid 117.

Molecular analysis and Secondary structure prediction.

Domain analysis of the SrABH protein revealed a significant similarity to the conserved alpha/beta hydrolase domain superfamily (within, pfam00561). This domain spans amino acids 38 to 278, with an E-value of 2.02e-25 (Figure 3).

Taxonomic analysis of SrABH at the protein level revealed 128 homologous sequences within the phylum Nematoda, of which 84 belonged to the order *Rhabditida*. Notably, 4 of these sequences were belonged to the *Strongyloidoidea* family and exhibited the highest similarity scors, including two hits derived from *S. ratti*, with a maximum score of 593. In contrast, nucleotide level analysis identified only a single hit. This finding further supports the phylogenetic placement of SrABH within the nematodes.

Secondary Structure and three-dimensional Modeling of SrABH.

Secondary structure prediction of the SrABH protein was performed using the PSIPRED program, which assigns structural elements, alpha, helices, beta sheets, and loops, using a seven-amino acid window. This approach allows for high-confidence predictions of amino acid positions based on structural probability calculations. Based on this analysis, both the secondary structure model (Figure 4A) and a three-dimensional (3D) structure model (Figure 4B) were generated. The 3D structure revealed a folded core characteristic of the alpha/beta hydrolase domain, containing 9 alpha helices and 8 beta sheets. Using PSIPRED, the SrABH protein was determined to consist of 39.18% alpha helices, 18.21% beta sheets, and 42.61% loop regions. The 3D structural modeling was based on 258 amino acids, representing 89% of the total coding sequence, and was generated with a confidence level of 99.99%. The modeled structure showed close similarity to the GenBank c7c4dA transcript. The protein was ultimately classified as a hydrolase enzyme.

Analysis of the N-terminal region of the SrABH protein using the TargetP-2.0 program identified the presence of a mitochondrial transfer peptide (mTP) with a confidence score of 0.9558. The predicted cleavage site was located between amino acids 21 and 22, corresponding to the motif RLF-SS (Figure 5).

Phylogenetic analysis and genetic distance

phylogenetic analysis of SrABH was conducted using amino acid sequence, from 18 parasitic nematode species. The SrABH sequence was positioned in cluster A, together with other nematode parasite sequences, supported by a high bootstrap value of 98 (Figure 6). Within this cluster, SrABH formed a distinct sub-cluster exclusively with the only available *S. ratti* protein sequence (XP_024505975). In contrast, all filarial nematode sequences grouped within cluster B, supported by a bootstrap value of 74. To ensure accurate phylogenetic placement, *Azospirillum agri-*

```
ATG TTT TGT AAA TCA CTT TCT TCA TCA TTG TTA TTT CGT AAC ATC CTC TCT CAG CGC CTA  60
 M   F   C   K   S   L   S   S   S   L   L   F   R   N   I   L   S   Q   R   L
TTT TCT TCA CTT TCT TAT ACA AAA TAT GGA GAA TGT TCT AAT ACT AGT CTT CCA CCA CTC 120
 F   S   S   L   S   Y   T   K   Y   G   E   C   S   N   T   S   L   P   P   L
TTG ATT GCT CAT GGT CTT TTT GGA AAC AAA AAA AAT TGG CAC TCT GCA GCA AAA GCA CTT 180
 L   I   A   H   G   L   F   G   N   K   K   N   W   H   S   A   A   K   A   L
CAA AAA AAA TTA GAC AAT CAA ATA TAT ACT ATT GAT CTT AGA AAT CAT GGA GAT AGT CCA 240
 Q   K   K   L   D   N   Q   I   Y   T   I   D   L   R   N   H   G   D   S   P
CAT TTA GAT TCA ATG ACT TAT CAA GAA ATG GCA GAA GAT GTG AAT AAT TTT ATA ACA AAT 300
 H   L   D   S   M   T   Y   Q   E   M   A   E   D   V   N   N   F   I   T   N
ATA ATT TTT GAA GAA ACA GGA TAC GAT GAA TTA GAT CTT TTG GGA CAT TCT ATG GGT GGT 360
 I   I   F   E   E   T   G   Y   D   E   L   D   L   L   G   H   S   M   G   G
AAA GTA AGT ATG GAA TTA GCT TTT AAC AAA GAA AGT TCA AAA AAT ATA AGA AAA TTA ATT 420
 K   V   S   M   E   L   A   F   N   K   E   S   S   K   N   I   R   K   L   I
ATT GAA GAT ATT TCA CCA ATT TAT GTT AAT AAA ACT CAT TTA TTT CCT AAA TAT ATT AAA 480
 I   E   D   I   S   P   I   Y   V   N   K   T   H   L   F   P   K   Y   I   K
GCT TTA ATG AAT ATT GAT TAT TCA TTA AGT CGT ATA GAA ATT GAT AAT ATT CTT AAA AAA 540
 A   L   M   N   I   D   Y   S   L   S   R   I   E   I   D   N   I   L   K   K
GAT ATT ACT GAT AAT GCT ACA AGA GCA TTC CTT TTG ACA AAC TTA CAA AAA GAC CAA GGT 600
 D   I   T   D   N   A   T   R   A   F   L   L   T   N   L   Q   K   D   Q   G
GCA GAA AGT TTT AGA TTT AAA GCA AAT TTA AAA AGT ATT AAT GAA TAT GTA GAT CAT ATT 660
 A   E   S   F   R   F   K   A   N   L   K   S   I   N   E   Y   V   D   H   I
ATA GGA TAC ACT TTT GAA AAA GGT TGT CAA TTT GAA AAA GAA ACT CTT TTT TTA TCA GGA 720
 I   G   Y   T   F   E   K   G   C   Q   F   E   K   E   T   L   F   L   S   G
GAA CAT TCA TTA TAT GTT ACT CCT AAT GAT AGA AAT TTA ATA AGA CGA TAC TTT CCT AAT 780
 E   H   S   L   Y   V   T   P   N   D   R   N   L   I   R   R   Y   F   P   N
GTT ACT TTT AAA GTT ATT GAA AAT TCA GGA CAT TGG ATA CAT GCC GAA CAT TTT CCT GCT 840
 V   T   F   K   V   I   E   N   S   G   H   W   I   H   A   E   H   F   P   A
TTC AAA GAA GCT GTT GTT TCA TTT TTA AAA AGT TAG ataaatttttattattaagaaattttacaataa 908
 F   K   E   A   V   V   S   F   L   K   S   .
tttacacatag                                                                    919
```

Figure 3.
Assembled Nucleotide Sequence of SrABH from S. ratti and Its Predicted Primary Structure. The coding sequence is represented in uppercase letters, whereas the 3'-untranslated regions are displayed in lowercase. Primer sites are underlined. Asn-Xaa-Ser/Thr motifs in the sequence are highlighted in gray. Asparagines predicted to undergo N-glycosylation are bolded and marked with a star. The most conserved protein region is boxed, with a serine residue active site in the center, indicated in bold.

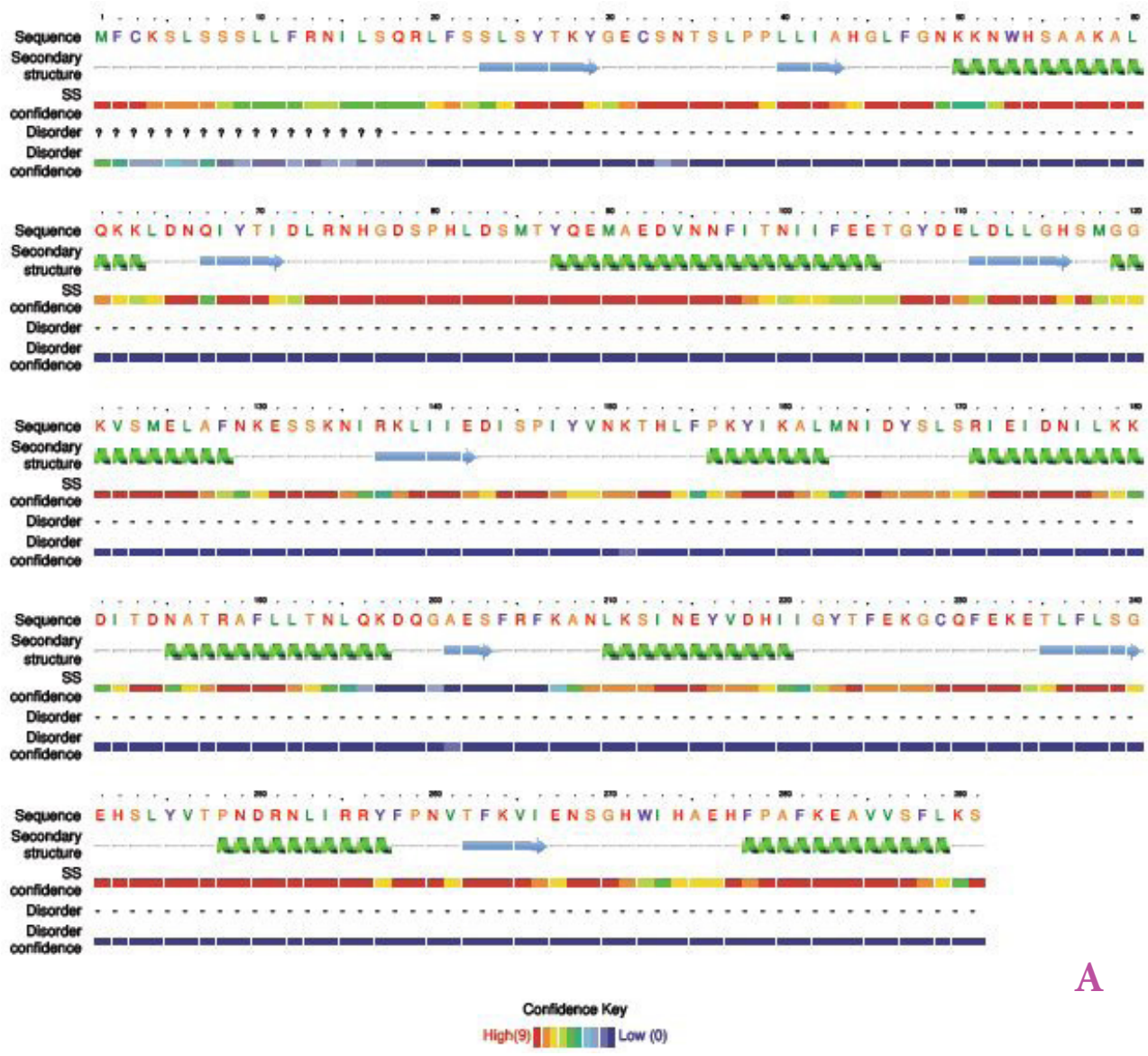

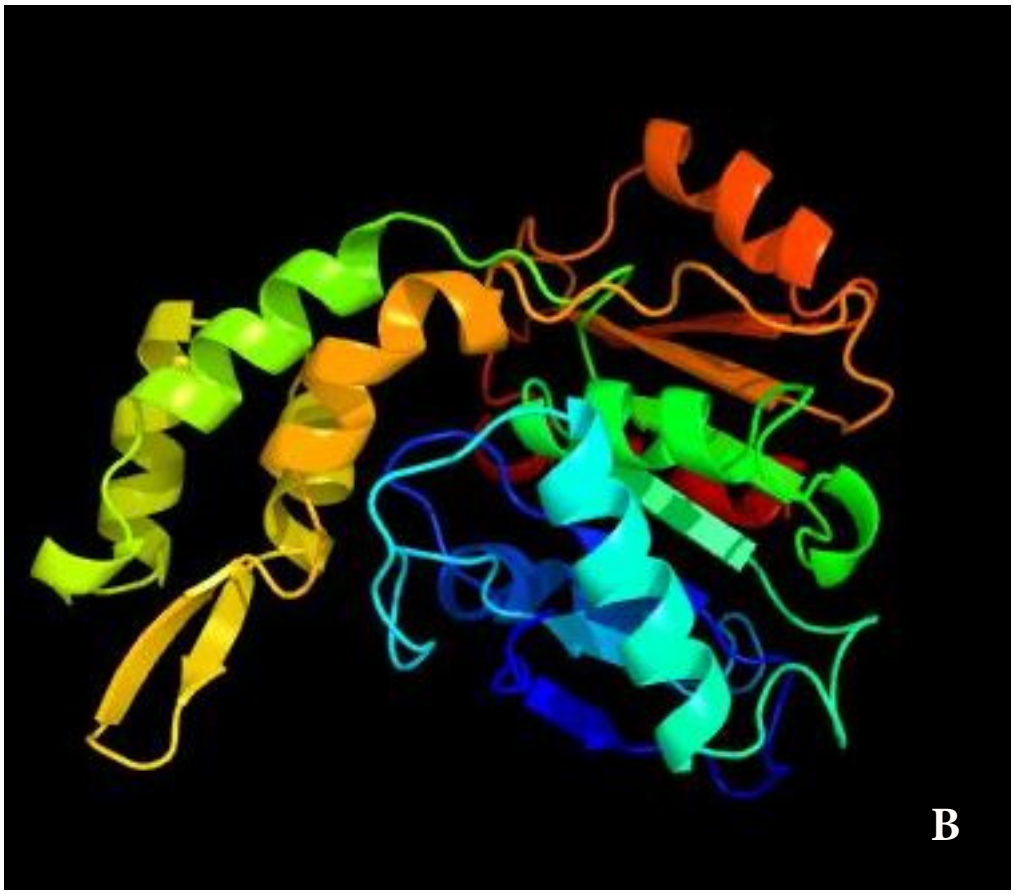

Figure 4.
Predicted secondary structure (A) and three-dimensional (3D) model (B) of the SrABH protein. Confidence levels for the secondary structure are color-coded, with red indicating high confidence and purple indicating low confidence.

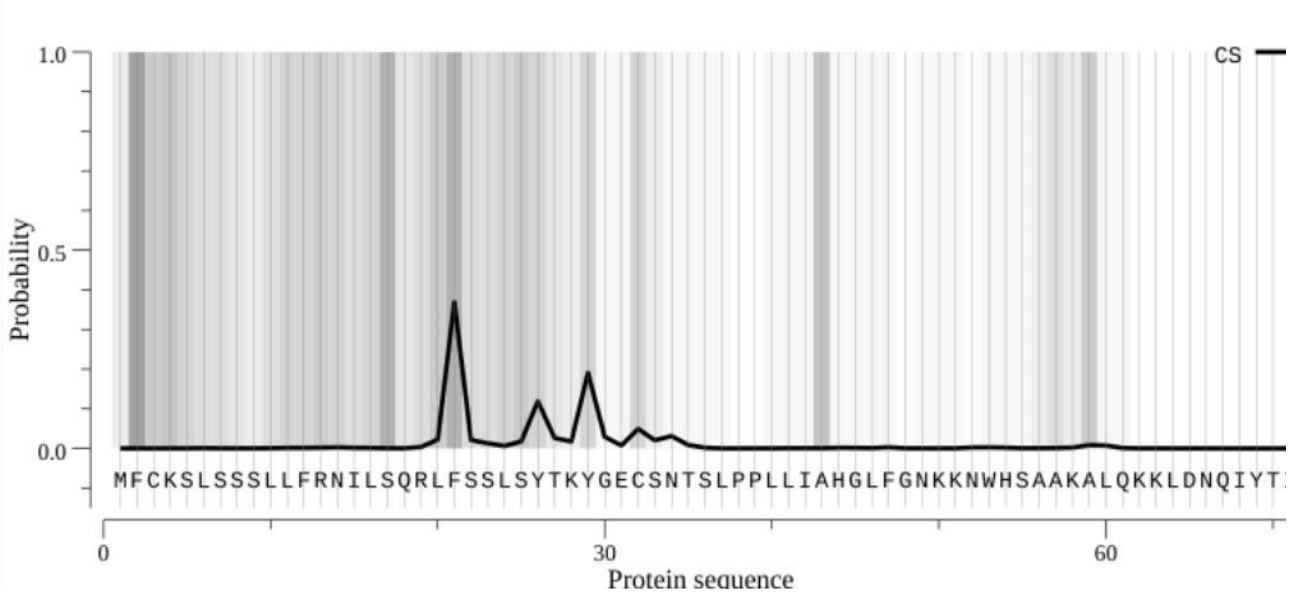

Figure 5.
Analysis of the N-terminal region of the SrABH protein, highlighting the predicted mitochondrial transfer peptide (mTP).

cola (WP_085556886.1) was used as an outgroup sequence.

Genetic analysis was performed using MEGA7 software, comparing SrABH with 12 nematode protein sequences retrieved from GenBank. SrABH sequence exhibited the lowest genetic distance (0.08%) relative to only known *S. ratti* protein sequence (XP_024505975) (Table 1). Genetic distance between SrABH and other related nematode species ranged from 5.2% to 5.7%, indicating notable sequence divergence within this family.

Discussion

Parasitic worms exhibit complex mechanisms for coexisting within their hosts across diverse environments [21]. One of the most effective survival mechanisms employed by these organisms is the secretion of excretory/secretory proteins, which play a central role in suppressing host immune response [22]. With advancements in *S. ratti* genome analysis, particularly the expansion of its Expressed Sequence Tags (ESTs) datasets, has significantly enhanced opportunities for molecular investigations. From a therapeutic perspective, a strategic and rational approach for development of anti-parasitic drugs, involves exploiting metabolic differences between parasites and their hosts to design specific enzyme inhibitors.

Among potential molecular targets, alpha/beta hydrolase proteins, which are widely conserved across all organisms [23], have been proposed as promising candidates for parasite-specific drug development. Despite this, no structural characterization of this protein has been reported in *S. ratti*. While several studies have reported alpha/beta hydrolase domain sequences in mammals, the complete cDNA sequence of this gene remained unknown in *S. ratti*.

The present study aimed to identify and characterize the protein from infected *S. ratti* larvae. Given

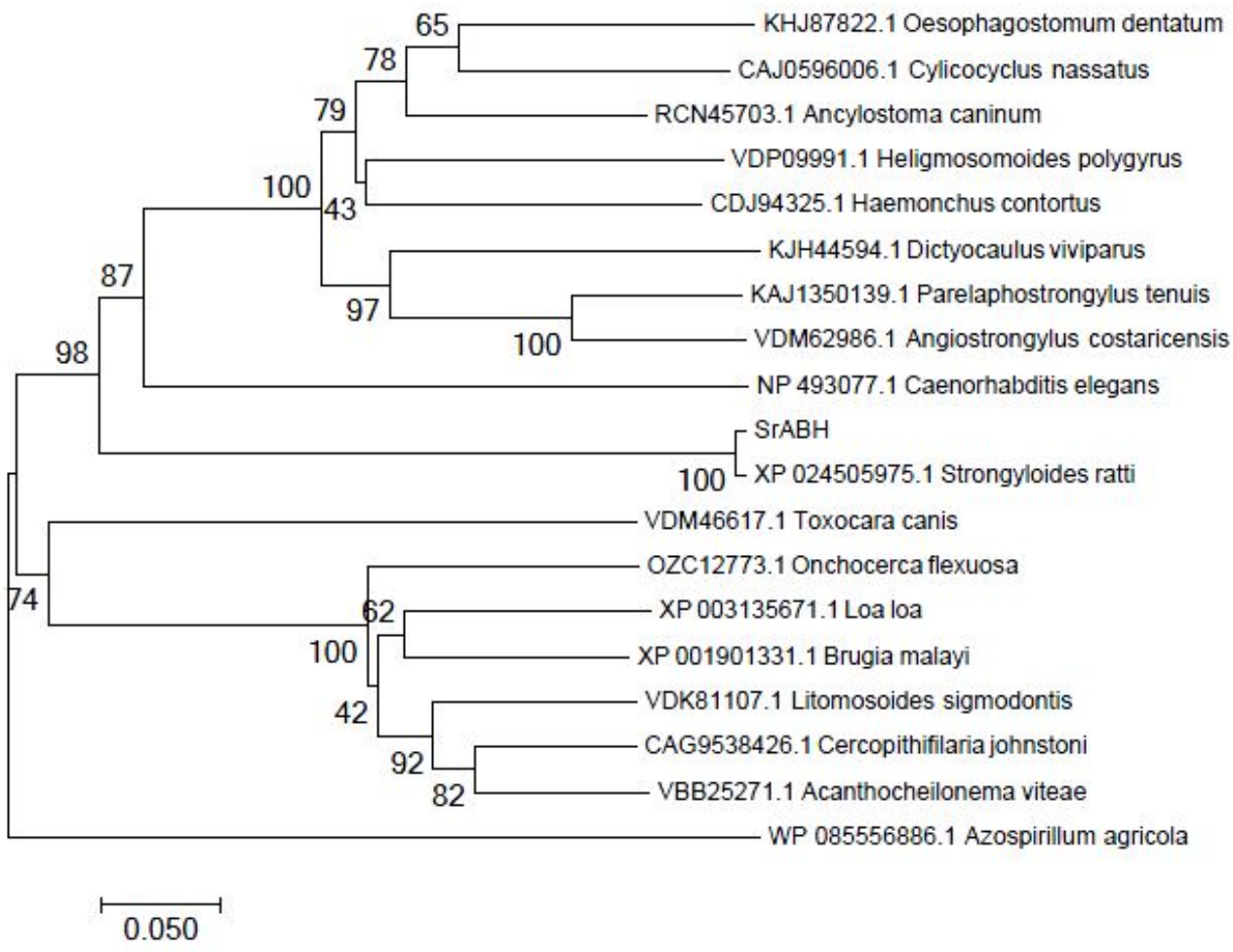

Figure 6.
Phylogenetic analysis of SrABH protein sequences and homologs using the Neighbor-Joining technique. Bootstrap values are derived from 1,000 replicates. Numbers preceding species names represent GenBank accession numbers, while numbers above the branches indicate phylogenetic relationships between groups.

Table 1.
The genetic pairwise distances of *Sr*ABH compared to the related *S. ratti* protein sequences

	1	2	3	4	5	6	7	8	9	10	11	12
1- SrABH												
2-XP_024505975.1 S. ratti	0.008											
3-RCN45703.1 A. caninum	0.528	0.524										
4-VDP09991.1_H. polygyrus	0.520	0.520	0.272									
5-NP_493077.1 C. elegans	0.537	0.537	0.480	0.504								
6-KHJ87822.1 O. dentatum	0.573	0.573	0.215	0.350	0.520							
7-CAJ0596006.1 C. nassatus	0.561	0.561	0.244	0.301	0.472	0.232						
8-CDJ94325.1 H. contortus	0.549	0.553	0.272	0.280	0.467	0.317	0.264					
9-KAJ1350139.1 P. tenuis	0.545	0.541	0.321	0.341	0.533	0.354	0.366	0.366				
10-VDM46617.1 T. canis	0.561	0.561	0.545	0.565	0.577	0.537	0.577	0.577	0.573			
11-KJH44594.1 D. viviparus	0.565	0.561	0.329	0.378	0.520	0.370	0.382	0.362	0.289	0.577		
12-VDM62986.1 A. costaricensis	0.561	0.565	0.317	0.350	0.516	0.337	0.366	0.386	0.146	0.545	0.333	
13-WP_085556886.1 A. agricola	0.630	0.630	0.602	0.593	0.638	0.614	0.638	0.622	0.630	0.581	0.630	0.622

that only a partial mRNA sequence was available in GenBank, we employed a combined strategy involving RT-PCR amplification and analysis of genomic and transcriptomic GenBank database to reconstruct the complete sequence, ensuring a more comprehensive understanding of its structural and functional characteristics. To amplify cDNA fragments encoding this gene, PCR was performed using cDNA as a template. Additionally, an Expressed Sequence Tag (EST) search strategy was employed to reconstruct the full-length cDNA by identifying overlapping regions. Subsequent multiple sequence alignment and phylogenetic analysis confirmed that SrABH possesses the alpha/beta hydrolase domain and belongs to the hydrolase enzyme family.

Although the precise cellular functions of hydrolase family proteins in parasitic nematodes remain poorly defined, accumulating evidence suggests that they play fundamental role in host-parasite interactions. For example, a member of this protein family has been identified as a key regulator of programmed cell death in *Arabidopsis thaliana* (24). Other studies have proposed that this gene may participate in cellular stress response pathways or function as a transcriptional factor (23, 25), although their molecular and cellular mechanisms are not yet fully understood. Notably, a component of the excretory/secretory material isolated from *Haemonchus contortus* has been classified as an alpha/beta hydrolase domain protein, where it has been shown to interact with host T cells [5]. By comparing the role of SrABH protein with HcABHD protein in H. contortus, particularly the HcABHD involvement in cell proliferation and apoptosis, it is likely that SrABH plays a similar function in the critical regulation of the cell cycle and host cell survival. A homologous protein, ABHD10, has been characterized in humans [26], and shown to consist of 306-amino acid [27]. This protein was identified alongside ABHD11, another mitochondrial-targeting protein isolated from human skeletal muscle mitochondria [27]. Additionally, ABHD11 has been reported to be enriched in the mitochondrial fraction of BV-2 mouse microglial cells [28]. Further analysis of the N-terminal region of SrABH revealed the absence of a signal peptide, suggesting that the protein is not secreted and instead functions intracellularly. Importantly, TargetP-2.0 analysis of SrABH predicted the presence of a mitochondrial transfer peptide (mTP) with high confidence, supporting its potential mitochondrial localization. Mitochondrial localization signal (MLS), also referred to as mitochondrial targeting sequence (MTS), are short peptides generally ranging from 15 to 70 amino acids and are enriched in positively charged residues. These sequence may play a critical role in protein trafficking to mitochondria [29]. Moreover, the three-dimensional (3D) structure of SrABH exhibits a balanced alpha/beta domain arrangement, characteristic of proteins within this family. Its core structure consists of beta sheets flanked by alpha helices, forming a stable fold.

The predicted structure, consisting of 9 alpha helices and 8 beta sheets, forms a well-defined catalytic domain that supports a diverse range of enzymatic functions, including mitochondrial targeting for intracellular protein transport, energy regulation, and protein degradation.

Consistent with these structural features, ScanProsite analysis identified the highly conserved motif centered on a serine residue (Figure 2). This residue, along with histidine and aspartic acid, as catalytic triad is known to participate in a catalyzing the substrate cleavage efficiently [30]. Similar conserved motifs have been reported in prokaryotic lipases and lecithin cholesterol acyltransferase (EC 2.3.1.43), which facilitates fatty acid transport among phosphatidylcholine and cholesterol [31].

In conclusion, SrABH plays a significant role in cellular processes regulating mitochondrial protein transport.

These findings provide valuable insights in understanding the function of this protein and pave the way for utilizing this knowledge in a structure-based drug design strategy and exploration of potential therapeutic interventions, particularly within a model system for human *S. stercoralis*.

Materials & Methods

Declaration of Generative AI and AI-assisted technologies in the writing process

Manuscript writing was done without the use of artificial intelligence tools.

S. ratti life cycle.

S. ratti were maintained by serial passage in male Wistar rats (Charles River). Infective third stage larvae (iL3) were obtained from fecal culture as previously described [14].

Total RNA isolation and cDNA Synthesis

Total RNA was isolated from 100,000 *S. ratti* infective third stage (iL3) larvae using RNX Plus solution (Cinagen, Iran), following the manufacturer's guidelines.

For cDNA synthesis, 2 µg of total RNA was incubated with 0.5 µg of oligo(dT) primer at 70°C for 10 minutes and immediately chilled on ice. Subsequently, 1 µl of RNasin (Cinagen, Iran), 1 µl of a 120 mM dNTP mixture (each nucleotide), 2.5 µl of 5× reaction buffer, and 1 µl (200 units) of Moloney Murine Leukemia Virus (M-MulV) reverse transcriptase were added. CDNA synthesis was carried out using the RevertAid First Strand cDNA Synthesis Kit (Thermo Fisher Scientific, USA) in accordance with the manufacturer's protocol. The reaction was incubated at 42°C for 1 hour, and subsequently finally inactivated at 70°C.

RT-PCR amplification

RT-PCR amplification was performed using primers ABH-F (5'-AACATCCTCTCTCAGCGCCTATTT) and ABH-R (5'-AGCAGGAAAAATGTTCGGCATGTA). Primers design was carried out using Primer3Plus software, based on the only available incomplete *S. ratti* mRNA sequence (XM_024650090.1) in GenBank. Each PCR reaction contained 5 µL of cDNA template, 0.2 µM of each primer, 250 µM of each dNTP, and 0.5 units of *Taq* DNA polymerase in a standard PCR buffer. Amplification was performed under the following cycling conditions: an initial denaturation at 94°C for 3 min, followed by 30 cycle of denaturation at 94°C for 30 seconds, annealing at 56°C for 30 seconds, and extension at 72°C for 1 min, with a final polymerization at 72°C for 7 min. PCR reactions were carried out using an Eppendorf Mastercycler Nexus Thermal Cycler (Eppendorf AG, Germany). Amplified products were analyzed by electrophoresis on a 1% agarose gel.

DNA sequence analysis

PCR products were sequenced using the original PCR primers with the BigDye Terminator v3.1 Cycle Sequencing Kit (Applied Biosystems, Foster City, CA, USA), and analyzed on an Applied Biosystems 3130 Genetic Analyzer (Applied Biosystems). Sequence assembly was performed by aligning overlapping fragment, and primers were designed using the Primer3 program. To evaluate evolutionary relationships, the sequences were compared with existing data in NCBI GenBank using the BLASTn algorithm.

Assembled nucleotide sequences were compared with existing sequences in the NCBI GenBank using the BLASTn algorithm to assess evolutionary relationships. Target sequences from other species were retrieved from NCBI GenBank, and signal peptide prediction was conducted using SignalP software [15] (cbs.dtu.dk/services/SignalP). Multiple sequence alignments were generated using CLUSTAL_W [16], and CDD-Search software from NCBI was employed to identify conserved domains [17]. The molecular weight (MW) and isoelectric point (pI) of the amino acid sequences were calculated using Expasy tools (ca.expasy.org/tools). Secondary structure prediction of the protein was performed using the PSIPRED protein sequence investigation (bioinf.cs.ucl.ac.uk/psipred) [18]. Mitochondrial transfer peptides at the N-terminus were predicted using TargetP-2.0 software (services.healthtech.dtu.dk/services/TargetP-2.0). Three-dimensional (3D) structure prediction was performed using Phyre2 server [19]. Phylogenetic analysis along and genetic distance calculations were performed using the neighbor-joining method with 1,000 bootstrap replicates in MEGA7 software [20]. Protein statistical parameters were analyzed using the Gene Infinity program (org/sms/sms_proteinstats.html). Protein domains were further examined using the ScanProsite tool (prosite.expasy.org/scanprosite), and N-glycosylation site was predicted using NetNGlyc 1.0 (http://www.cbs.dtu.dk/services/NetNGlyc).

Authors' Contributions

A.J. conceived and planned the experiments. A.J. carried out the experiments. A.J. planned and carried out the simulations. A.J. Contributed to sample preparation. A.J. contributed to the interpretation of the results. A.J. took the lead in writing the manuscript. All authors provided critical feedback and helped shape the research, analysis and manuscript.

Acknowledgements

This work was financially supported by research grant from the Vice President of the Research Affairs

Office at the Shahid Chamran University of Ahvaz, Ahvaz- Iran.

Conflict of interest

The authors declare that there is no conflict of interest.

References

1. Buonfrate D, Bisanzio D, Giorli G, Odermatt P, Furst T, Christina Greenaway C. The global prevalence of Strongyloides stercoralis infection. Pathogens. 2020; 9:468. Doi: 10.3390/pathogens9060468.

2. Nemetschke L, Eberhardt AG, Viney ME, Streit A. A genetic map of the animalparasitic nematode Strongyloides ratti. Mol Biochem Parasitol. 2010;169:124-127. Doi:10.1016/j.molbiopara.2009.10.008.

3. Luciana PS, Solange da Costa Barcelos I. Passos-Lima AB, Espindola FS, Barbosa Campos DM, Costa-Cruz JM (2003) Western blotting using strongyloides ratti antigen for the detection of IgG antibodies as confirmatory test in human strongyloidiasis. Mem Inst Oswaldo Cruz. 2003;98(5):687-91. Doi:10.1590/s0074-02762003000500017.

4. Holmquist M. Alpha/Beta-hydrolase fold enzymes: structures, functions and mechanisms. Curr Protein Pept Sci. 2000; 1(2):209-35. Doi:10.2174/1389203003381405.

5. Lu M, Tian X, Tian AL, Li C, Yan R, Xu L, et al. A Novel α/β Hydrolase Domain Protein Derived from Haemonchus contortus Acts at the Parasite-Host Interface. Front Immunol. 2020; 30(11):1388. Doi: 10.3389/fimmu.2020.01388.

6. Moreno Y, Gros PP, Tam M, Segura M, Valanparambil R, Geary TG. Proteomic analysis of excretory-secretory products of Heligmosomoides polygyrus assessed with next-generation sequencing transcriptomic information. PLOS Neglected Tropical Diseases. 2011;5:e1370. Doi: 10.1371/journal.pntd.0001370.

7. Vendelova E, de Lima JC, Lorenzatto KR, Monteiro KM, Mueller T, Veepaschit J. Proteomic analysis of excretory-secretory products of Mesocestoides corti metacestodes reveals potential suppressors of dendritic cell functions. PLOS Neglected Tropical Diseases. 2016;10:e0005061. Doi: 10.1371/journal.pntd.0005061.

8. Xie M, Roy R. The causative gene in chanarian dorfman syndrome regulates lipid droplet homeostasis in C. elegans. PLoS Genetics. 2015;11: e1005284. Doi:10.1371/journal.pgen.1005284.

9. Guo F, Zhang H, Eltahan R, Zhu G. Molecular and biochemical characterization of a type II thioesterase from the zoonotic protozoan parasite Cryptosporidium parvum. Frontier in cellular and infection microbiology. 2019; 9:199. Doi: 10.3389/fcimb.2019.00199.

10. Fan J, Yang W, Brindley PJ. Lysophospholipase from the human blood fluke, Schistosoma japonicum. International Journal of Infectious Diseases. 2008;12:143-51. Doi: 10.1016/j.ijid.2007.05.005.

11. Vijayakumar A, Vijayaraj P, Vijayakumar AK, Rajasekharan R. The Arabidopsis ABHD11 mutant accumulates polar lipids in leaves as a consequence of absent acylhydrolase activity. Plant Physiology. 2016;170:180-93. Doi: 10.1104/pp.15.01615.

12. Park S, Gidda SK, James CN, Horn PJ, Khuu N, Seay DC. The a/b hydrolase CGI-58 and peroxisomal transport protein PXA1 coregulate lipid homeostasis and signaling in Arabidopsis. Plant Cell. 2013;25:1726-39. Doi: 10.1105/tpc.113.111898.

13. Ghosh AK, Ramakrishnan G, Chandramohan C, Rajasekharan R. CGI-58, the causative gene for Chanarin-Dorfman syndrome, mediates acylation of lysophosphatidic acid. Journal of Biological Chemistry. 2008;83:24525-33. Doi: 10.1074/jbc.M801783200.

14. Keiser J, Thiemann K, Endriss Y, Utzinger J. Strongyloides ratti: in vitro and in vivo activity of tribendimidine. PLoS Negl Trop Dis. 2008;23;2(1):e136. DOI:10.1371/journal.pntd.0000136.

15. Nielsen H, Engelbrecht J, Brunak S, von Heijne, G. (1997). Identification of prokaryotic and eukaryotic signal peptides and prediction of their cleavage sites. Protein Engineering. 1977;10:1-6. Doi: 10.1093/protein/10.1.1.

16. Thompson JD, Higgins DG, Gibson TJ. CLUSTAL W: improving the sensitivity of progressive multiple sequence alignment through sequence weighting, position-specific gap penalties and weight matrix choice. Nucleic Acids Research. 1994;22:4673-4680. Doi: 10.1093/nar/22.22.4673.

17. Marchler-Bauer A. CDD/SPARCLE: functional classification of proteins via subfamily domain architectures. Nucleic Acids Research. 2017 45:200-203. Doi: 10.1093/nar/gkw1129.

18. Buchan DWA, Moffat L, Lau A, Kandathil SM, Jones DT. Deep learning for the PSIPRED Protein Analysis Workbench Nucleic Acids Research. 2024; 52:287-293. Doi:10.1093/nar/gkae328.

19. Kelley LA, Sternberg MJE (2009) Protein structure prediction on the Web: a case study using the Phyre server, Nature protocols. 2009;4(3):363-71. Doi:10.1038/nprot.2009.2. PMID:19247286.

20. Tamura K, Dudley J, Nei M, Kumar S. MEGA4: Molecular Evolutionary Genetics Analysis (MEGA) software version 4.0. Molecular Biology and Evolution. 2007;24: 1596-1599. Doi: 10.1093/molbev/msm092.

21. Harris NL. Recent advances in type-2-cell-mediated immunity: insights from helminth infection. Immunity. 2017 47: 1024-36. Doi: 10.1016/j.immuni.2017.11.015.

22. Ditgen D, Anandarajah EM, Reinhardt A, Younis AE, Witt S, Hansmann J, et al. Comparative characterization of two galectins excreted-secreted from intestine-dwelling parasitic versus free-living females of the soil-transmitted nematode Strongyloides. Mol Biochem Parasitol. 2018; 225:73-83. Doi: 10.1016/j.molbiopara.2018.08.008.

23. Sun J, Zhang D, Bae DH, Sahni S, Jansson P, Zheng Y. Metastasis suppressor, NDRG1, mediates its activity through signaling pathways and molecular motors. Carcinogenesis. 2013; 34:1943-1954. Doi: 10.1093/carcin/bgt163. PMID 23671130.

24. Shapiro AD, Chu Zhang C. The Role of NDR1 in Avirulence Gene-Directed Signaling and Control of Programmed Cell Death in Arabidopsis. Plant Physiology. 2001;127:1089-1101. Doi: 10.1104/pp.010096.

25. Fang BA, Kovacevic Z, Park KC, Kalinowski DS, Jansson PJ, Lane DJ, et al. Molecular functions of the iron-regulated metastasis suppressor, NDRG1, and its potential as a molecular target for cancer therapy. Biochimica et Biophysica Acta. 2014;1845:1-19. Doi: 10.1016/j.bbcan.2013.11.002.

26. Lord CC, Thomas G, Brown JM. Mammalian alpha beta hydrolase domain (ABHD) proteins: Lipid metabolizing enzymes at the interface of cell signaling and energy metabolism. Biochim Biophys Acta. 2013;1831(4):792-802. Doi: 10.1016/j.bbalip.2013.01.002. PMID: 23328280.

27. Lefort N, Yi Z, Bowen B, Glancy B, De Filippis EA, Mapes R, et al. Proteome profile of functional mitochondria from human skeletal muscle using one-dimensional gel electrophoresis and HPLC-ESI-MS/MS. J Proteomics. 2009; 72:1046-1060.

28. Marrs WR, Blankman JL, Horne EA, Thomazeau A, Lin YH, Coy J, Bodor AL, et al. The serine hydrolase ABHD6 controls the accumulation and efficacy of 2-AG at cannabinoid receptors. Nat Neurosci. 2010; 13:951-957. PubMed: 20657592.

29. Li M, Zhong Z, Zhu J, Xiang D, Dai N, Cao X, et al. Identification and characterization of mitochondrial targeting sequence of human apurinic/apyrimidinic endonuclease 1. J Biol Chem. 2010;285(20):14871-14881.Doi:10.1074/jbc.M109.069591. PMID: 20231292.

30. Blow D. Enzymology. More of the catalytic triad. Nature. 1990 ; 22: 343(6260): 694-5. Doi: 10.1038/343694a0. PMID: 2304545.

31. McLean J, Fielding C, Drayna D, Dieplinger H, Baer B, Kohr W, et al. Cloning and expression of human lecithin-cholesterol acyltransferase cDNA. Proc Natl Acad Sci U S A. 1986; 83(8): 2335-9. Doi: 10.1073/pnas.83.8.2335.

How to cite this article
Jolodar A. Characterization and phylogenetic analysis of a mitochondrial targeting alpha/beta hydrolase protein in *Strongyloides ratti*. Iran J Vet Sci Technol.2026; 18(1): 61-70.
DOI: https://doi.org/10.22067/ijvst.2025.93653.1549
URL: https://ijvst.um.ac.ir/article_47555.html